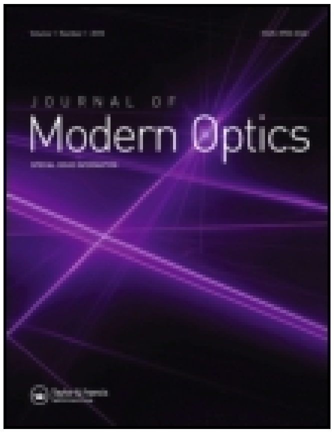

Journal of Modern Optics
Publication details, including instructions for authors and subscription information:
http://www.tandfonline.com/loi/tmop20

Multicore photonic-crystal-fiber platform for high-power all-fiber ultrashort-pulse sources

Ming-Lie Hu [a] , Xiao-Hui Fang [a] , Bo-Wen Liu [a] , Lu Chai [a] , Yan-Feng Li [a] , Aleksei M. Zheltikov [b c] & Ching-Yue Wang [a]

[a] Ultrafast Laser Laboratory, Key Laboratory of Opto-electronic Information Science and Technology of Ministry of Education , College of Precision Instruments and Opto-electronics Engineering, Tianjin University , 300072 Tianjin, P.R. China

[b] Department of Physics and Astronomy , Texas A&M University , College Station, TX 77843-3257, USA

[c] Physics Department , International Laser Center, M.V. Lomonosov Moscow State University , Moscow 119992, Russia

Published online: 27 Jul 2011.

Journal of Modern Optics
Vol. 58, No. 21, 10 December 2011, 1966–1970

Multicore photonic-crystal-fiber platform for high-power all-fiber ultrashort-pulse sources

Ming-Lie Hu[a], Xiao-Hui Fang[a], Bo-Wen Liu[a], Lu Chai[a], Yan-Feng Li[a],
Aleksei M. Zheltikov[b,c]* and Ching-Yue Wang[a]

[a]*Ultrafast Laser Laboratory, Key Laboratory of Opto-electronic Information Science and Technology of Ministry of Education, College of Precision Instruments and Opto-electronics Engineering, Tianjin University, 300072 Tianjin, P.R. China;* [b]*Department of Physics and Astronomy, Texas A&M University, College Station TX 77843-3257, USA;* [c]*Physics Department, International Laser Center, M.V. Lomonosov Moscow State University, Moscow 119992, Russia*

(*Received 28 February 2011; final version received 13 June 2011*)

Ytterbium-doped multicore photonic crystal fibers are shown to provide an advantageous platform for the phase-locked amplification of ultrashort light pulses, enabling the generation of sub-100 fs microjoule light pulses at repetition rates as high as 50 MHz.

Keywords: photonic crystal fiber; ultrashort pulse; phase-locked amplification

Large-mode-area (LMA) photonic crystal fibers (PCFs) [1,2] open new horizons in fiber-laser technology. Fibers of this type help suppress unwanted nonlinear optical effects in the regime of high laser energies, thus enabling the creation of high-power fiber lasers and amplifiers with a superb output beam quality [3,4]. Multiple-core LMA PCFs have been recently shown [5,6] to offer promising strategies for a further increase in the output power of fiber laser systems. Properly designed multicore PCFs can provide a larger mode area compared to single-core PCFs and reduce heat- and stress-induced beam distortions at high power levels. However, high beam quality of a multicore PCF output can be achieved only when the individual core outputs are phase locked [7–12]. Such phase locking can be achieved through the use of a Talbot cavity [7], structured mirrors [8], and spatial filtering [10]. In the regime of strong evanescent-field coupling of the fiber cores, in-phase supermode selection, as first demonstrated by Cheo et al. [9], can also occur spontaneously above a certain level of pump powers. Michaille et al. [10] have recently employed a six-core PCF to demonstrate the generation of 26 ns laser pulses with energies up to 2.2 mJ and a mode field area of 4200 μm^2 in the Q-switching regime. A digital-holography wave-front control of a 19-core ytterbium-doped fiber amplifier has been shown to enable efficient amplification of suppicosecond laser pulses [12]. Daniault et al. [13] have recently demonstrated coherent beam combining of two femtosecond fiber chirped-pulse amplifiers seeded with a common oscillator through the use of an electro-optical phase-modulator-based feedback loop.

Here, we show that multicore PCFs provide an advantageous platform for the solution of this problem, enabling the generation of sub-100 fs microjoule light pulses at repetition rates as high as 50 MHz. We present a fiber laser–amplifier system with an Yb-doped LMA-PCF laser, an LMA-PCF preamplifier, and a 7- or 18-core PCF amplifier, yielding a high-power fiber output compressible to ultrashort pulse widths. We also demonstrate that pulse compression of the multicore-PCF-amplifier output to shorter pulse widths, including few-cycle field waveforms, can be achieved through spectral broadening in LMA all-solid photonic band-gap fibers (PBGF), as well as through waveform synthesis using multiple wavelength-shifted solitons, dispersive waves emitted by solitons, and the third harmonic. Whereas some of the individual components of this platform, including a 7-core-PCF amplifier [5] and an all-solid-PCF pulse compressor [14], have been reported in our earlier work, here, we present for the first time the entire integrated system for the generation, amplification, pulse compression, as well as temporal and spectral transformation of ultrashort light pulses where all the key functional elements are based on different types of PCFs.

A typical scheme of a fiber laser with a multicore-PCF amplifier is shown in Figure 1. The master oscillator is based on an Yb-doped (with a ≈1000 ppm wt doping level) single-polarization double-clad LMA PCF with a core diameter of 29 μm. In the mode-locking regime, the PCF oscillator delivers 600 fs light pulses with a central wavelength of 1040 nm and an average power up to 400 mW at a repetition rate

*Corresponding author. Email: zheltikov@phys.msu.ru

ISSN 0950–0340 print/ISSN 1362–3044 online

http://dx.doi.org/10.1080/09500340.2011.597521
http://www.tandfonline.com

of 50 MHz. For the preamplifier, we employ a 3.5 m piece of an Yb-doped LMA PCF, which is identical to the fiber used in the oscillator. Pre-amplified pulses with an average power of 700 mW pass through an isolator and enter a multicore LMA PCF of the main amplifier. The multicore PCF is end-pumped by a fiber-coupled laser diode operating at 976 nm. A scheme with a counter-propagating pump was chosen in order to minimize the influence of nonlinear-optical effects. The output of the multicore PCF was compressed with a grating pair in a four-bounce configuration. Appropriate telescopic systems were used to image the oscillator and amplifier outputs on a beam analyzer (coherent) for near- and far-field measurements. Temporal and spectral characterization of the fiber-laser and fiber-amplifier output pulses were performed with a long scan-range autocorrelator (APE Pulse Check) and a high-resolution spectrometer (Ando 6315 A).

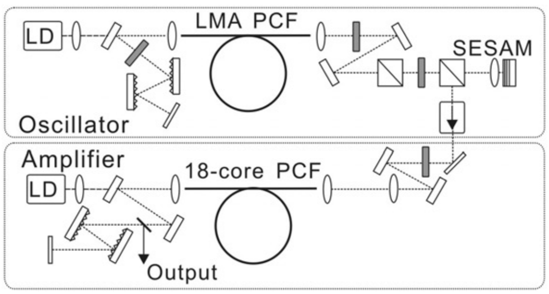

Figure 1. Diagram of the fiber source with an LMA PCF oscillator and multicore-PCF amplifier: LMA PCF, large-mode-area photonic-crystal fiber; SESAM, semiconductor saturable-absorber mirror; LD, photodetection system.

Photonic crystal fibers with 7 and 18 Yb-doped cores (Figure 2(*a*) and (*b*)) were used at the amplification stage. With an appropriate optimization of pump and fiber parameters [5,6], both types of fibers have been shown to support a robust phase-locked amplification of the preamplifier output, giving rise to smooth stable bell-shaped field intensity profiles in the far field. With the 7-core PCF, the 0.7 W, 1 MHz, 1.9 ps preamplifier output was amplified in the phase-locked regime to 24 W pulses, which were compressed with a grating compressor to 110 fs pulses with a peak power up to 150 MW. The 18-core PCF amplifier was capable of delivering pulses with a pulse width of about 80 fs (following pulse compression, Figure 3(*a*) and (*b*)) and a pulse energy of 1 μJ at a pulse repetition rate of 50 MHz.

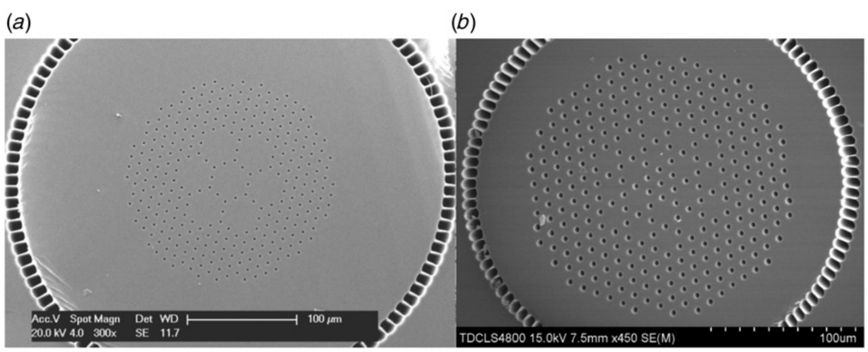

Figure 2. SEM images of 7-core (*a*) and 18-core (*b*) PCFs. In both types of PCFs, multiple fiber cores, seen in the central part of the fiber structure, are separated from each other by single-air hole-thick rings and are surrounded by a microstructure cladding. The scale bars seen in the lower parts of the images correspond to 100 μm.

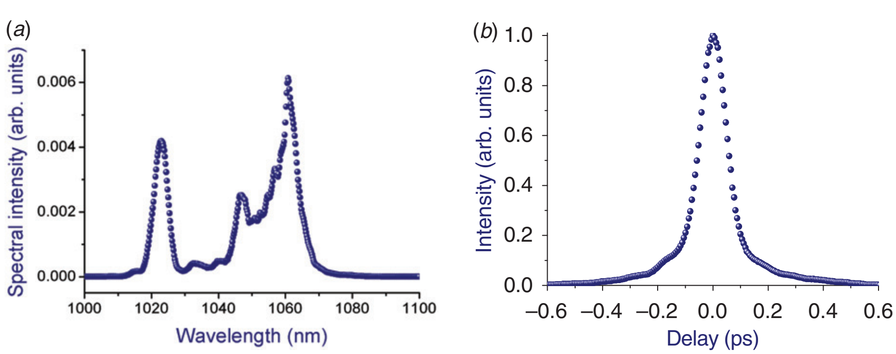

Figure 3. The spectrum (*a*) and autocorrelation trace (*b*) of the compressed output of the 18-core PCF amplifier. (The color version of this figure is included in the online version of the journal.)

Development of fiber-format solutions for the pulse compression of multicore-PCF-amplifier output calls for fiber components capable of supporting single-mode guiding of high-power laser pulses and providing careful control over the dispersion profile within a broad spectral range. Such a control can be attained with small-core PCFs, where the waveguide dispersion is tailored to balance material dispersion for a targeted dispersion profile within a broad frequency range. In a silica–air, 'holey' LMA PCF, this strategy of dispersion control is much less efficient, as the dispersion profile in such fibers is typically dominated by material dispersion. All-solid PCFs, also referred to as all-solid photonic band-gap fibers (PBGFs) [15], in many ways help to resolve this difficulty. In PCFs of this class, the light is guided along a silica core by antiresonance reflection from a periodic (photonic crystal) array of high-index strands in the fiber cladding. As a result, within a limited frequency band of antiresonance reflection, dispersion tailoring for such a fiber can be decoupled from mode-area engineering. All-solid PBGFs have been shown to offer attractive solutions for the generation of ultrashort pulses in mode-locked ytterbium-doped fiber lasers [16], spectral broadening [17,18], as well as for the compression of high-peak-power ultrashort laser pulses [19].

In our all-PCF source of ultrashort pulses, we use a homemade all-solid PBGF [14] with an effective mode area of about 110 μm^2 (see inset in Figure 4) and a dispersion profile designed to support soliton propagation within the range of wavelengths from approximately 1060 to 1400 nm to demonstrate a wavelength-tunable source of high-energy sub-100 fs light pulses. All the key components of this source, such as a master oscillator, an amplifier, and a tunable frequency shifter, are based on PCFs, with the all-solid PBGF serving to transform a 1040 nm, 50 MHz, 100 fs amplified output of a large-mode-area ytterbium-doped PCF oscillator-amplifier system into sub-100 fs, 6.4 nJ light pulses smoothly tunable within the range of wavelengths from 1160 to 1260 nm.

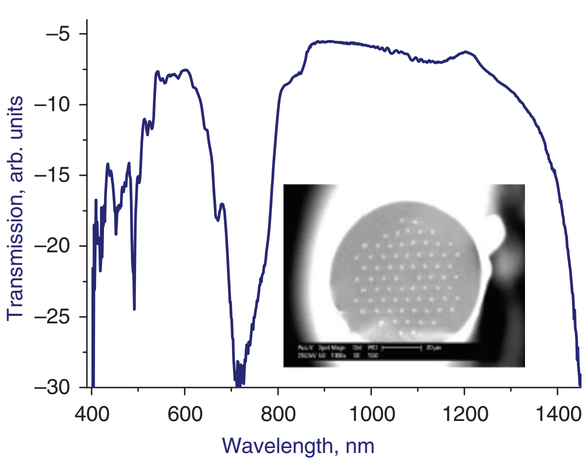

Figure 4. Transmission spectrum (on the logarithmic scale) of an all-solid photonic band-gap fiber with the cross-sectional structure shown in the inset. (The color version of this figure is included in the online version of the journal.)

The laser-oscillator and amplifier stages of the system employ diode-pumped ytterbium-doped single-polarization LMA PCFs in a stretcher-free configuration, delivering laser pulses with a central wavelength of 1040 nm and a maximum average power of 28 W at a pulse repetition rate of 50 MHz. An amplified LMA PCF laser output compressed to a pulse width of about 100 fs with a grating compressor was launched into an all-solid PCF. A silica cladding of this fiber includes a hexagonal periodic array of germanium-doped (≈20 mol. %) strands running along the fiber. The diameter of each Ge-doped inclusion in the fiber cladding is 2 μm, with the pitch of the hexagonal lattice formed by these inclusions being 6 μm. Material dispersion of germanium inclusions slightly modifies dispersion and nonlinearity of the resulting fiber structure. However, these effects are negligible compared to the influence of the photonic band gap (PBG), provided by a hexagonal periodic lattice of Ge-doped inclusions. A fiber structure with a PBG cladding can support waveguide modes that cannot be guided without a PBG cladding. Dispersion profiles of these PBG-guided modes are radically different from the dispersion profiles of index-guided modes. In particular, the zero-GVD wavelength can be shifted along with PBG shifting by varying the lattice constant of Ge-doped inclusions and the level of Ge doping.

The fiber is designed in such a way as to provide a broad transmission band around the central wavelength of our Yb-doped LMA PCF laser and to support a broadband wavelength tunability of solitons generated by the LMA PCF laser output. Spectrally resolved transmission measurements were performed by butt-coupling supercontinuum radiation from a highly nonlinear PCF into a 1 m section of the all-solid PBGF. The first transmission band of our all-solid PBGF stretches from 780 to 1400 nm (Figure 4). Spatially resolved measurements, performed by imaging a low-intensity 1040 nm LMA PCF laser beam transmitted through the fiber on a CCD camera, confirm that more than 95% of laser energy at the fiber output is concentrated in the fundamental mode of the fiber. The effective area of the fundamental mode of this fiber is estimated as 110 μm^2 at a wavelength of 1040 nm.

Figure 5 shows a map of the spectrally resolved PBGF output measured as a function of the average power of input 100 fs LMA PCF laser pulses. The central wavelength of input radiation falls within the range of normal fiber dispersion. As a result, for input

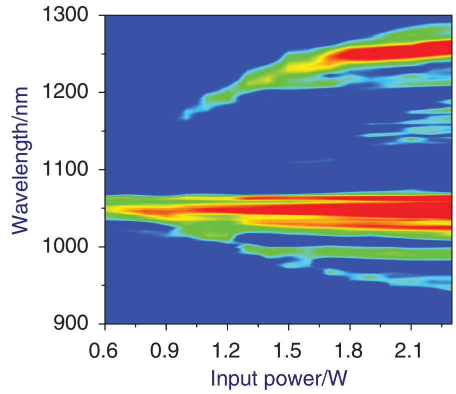

Figure 5. Spectrally resolved PBGF output measured as a function of the average power of input 100 fs 50 MHz LMA PCF laser pulses. The fiber length is 30 cm. An input average power of 1 W corresponds to a peak power of 0.2 MW. (The color version of this figure is included in the online version of the journal.)

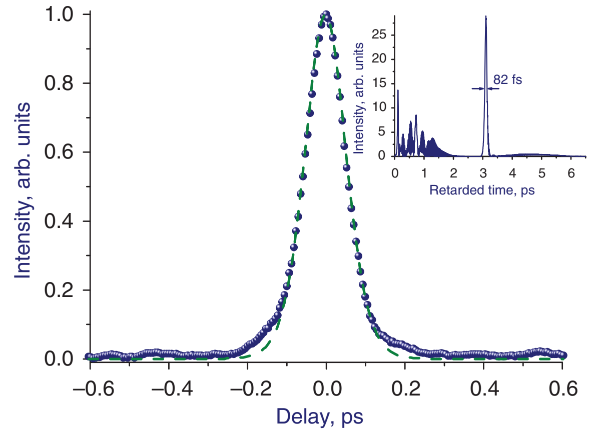

Figure 6. Autocorrelation trace of the spectrally filtered PBGF soliton output with a central wavelength of 1260 nm (filled circles) and a hyperbolic-secant-shaped pulse with a pulse width of 84 fs (dashed line). The inset shows the results of NLSE-based simulations for the spectrally filtered 1260 nm soliton at the output of the PBGF under the same conditions. (The color version of this figure is included in the online version of the journal.)

average powers below 0.9 W, no soliton formation is observed in the PBGF output. The spectral transformation of the LMA PCF pulses in this regime is dominated by self-phase modulation (SPM). For higher input powers (above 1 W in Figure 5(*a*)), SPM-induced spectral broadening starts to generate sufficiently intense spectral content in the region of anomalous fiber dispersion, giving rise to soliton formation. These solitons experience soliton self-frequency shift due to the Raman effect [20], leading to the generation of an intense red-shifted component in the PBGF output. As can be seen from Figure 5(*a*), the central wavelength of this component can be tuned from 1160 to 1260 nm by increasing the input laser power from 1 to 2.4 W.

With an appropriate spectral filter applied to select the wavelength-shifted soliton from the non-solitonic part of the field at the output of the PBGF, the maximum average power of the soliton with a central wavelength of 1260 nm was estimated as 320 mW, which corresponds to an energy of 6.4 nJ. The pulse width of this soliton was measured with the use of the autocorrelation technique. The measured autocorrelation trace of the soliton PBGF output (circles in Figure 6) only slightly deviates in its edges from an autocorrelation trace calculated for an ideal hyperbolic-secant-shaped soliton pulse with a pulse width of 84 fs (dashed line in Figure 6). This estimate for the soliton pulse width agrees well with the results of numerical simulations, predicting a pulse width of 82 fs for a frequency-shifted soliton with a central wavelength of 1260 nm (see inset in Figure 6).

Frequency-shifted solitons in highly nonlinear PCFs have been found to give rise to high-visibility interference fringes in PCF output spectra [21], indicating flat spectral phase profiles of individual solitons in the PCF output. This experimental finding, supported by numerical simulations, suggests a promising method of fiber-format pulse shaping and an attractive technology for few-cycle pulse synthesis through a coherent addition of frequency-shifted solitons generated in a highly nonlinear fiber.

To demonstrate the suitability of frequency-shifted solitons generated in a highly nonlinear fiber for the synthesis of few-cycle light pulses, we use a model based on a numerical solution of the generalized nonlinear Schrödinger equation (GNSE) [20]. This model includes [22] dispersion effects up to the ninth order, Kerr and Raman optical nonlinearity, as well as shock-wave phenomena. Simulations were performed for Gaussian light pulses with an input central wavelength of 1250 nm and an initial pulse width of 100 fs. Parameters of simulations have been chosen in such a way as to mimic LMA PCFs suitable for the generation of high-power solitons: an effective mode area of 20 μm^2, zero-GVD wavelength $\lambda_0 \approx$ 1000 nm, and high-order dispersion coefficients $\beta_3 = 7.6 \times 10^{-5}\,ps^3/m$, $\beta_4 = -9.4 \times 10^{-8}\,ps^4/m$, $\beta_5 = 2.5 \times 10^{-10}\,ps^5/m$, $\beta_6 = -1.2 \times 10^{-12}\,ps^6/m$. These numerical simulations fully support our main conclusions based on the analysis of experimental data. A laser pulse with a sufficiently high input peak power tends to split into multiple red-shifting solitons as it propagates through the fiber. At a sufficiently high level of input peak powers, the soliton spectra overlap, giving rise to interference fringes in the output spectrum. The simulated spectral and temporal field structure at the fiber output is accurately approximated by a superposition of five solitonic pulses with central frequencies $\nu_1 \approx 211$ THz, $\nu_2 \approx 198$ THz, $\nu_3 \approx 191$ THz, $\nu_4 \approx 164$ THz, $\nu_5 \approx 149$ THz, pulse widths $T_1 \approx 22$ fs, $T_2 \approx 27$ fs, $T_3 \approx 29$ fs, $T_4 \approx 30$ fs, $T_5 \approx 35$ fs, energies 1.6, 2.6, 2.9, 4.6, and 5.5 nJ, and delay times $\Delta_2 - \Delta_1 \approx 220$ fs, $\Delta_3 - \Delta_1 \approx 400$ fs, $\Delta_4 - \Delta_1 \approx 1080$ fs, and $\Delta_5 - \Delta_1 \approx 1890$ fs. With a light modulator generating an appropriate five-step group-delay profile [21], the solitons add up to synthesize a light pulse with a pulse width of about 10 fs. The total radiation energy of the compressed PCF output is 26.6 nJ, with the central, 10 fs part of the compressed pulse carrying an energy of 11.7 nJ.

We have demonstrated that multicore PCFs provide an advantageous platform for the solution of this problem, enabling the generation of sub-100 fs microjoule light pulses at repetition rates as high as 50 MHz. Fiber-format pulse compression of the multi-core-PCF-amplifier output to shorter pulse widths, including few-cycle field waveforms, can be achieved through spectral broadening in large-mode-area photonic band-gap fibers, as well as through waveform synthesis using multiple wavelength-shifted solitons, dispersive waves emitted by solitons, and the third harmonic. High-repetition-rate sub-100 fs microjoule multicore-PCF-based fiber sources demonstrated in this work are ideally suited as front-end systems for advanced extreme-power laser facilities and as flexible and compact, but still powerful tool for nonlinear imaging, micromachining, and laser surgery.

Acknowledgements

The authors are grateful to the Yangtze Optical Fiber and Cable Company Ltd. (Wuhan, China) for providing the all-solid PCF samples. Helpful discussions with A.B. Fedotov, D.A. Sidorov-Biryukov, and A.A. Voronin are gratefully acknowledged. This work was supported in part by National Basic Research Program of China (Grant No. 2011CB808101 and 2010CB327604), National Natural Science Foundation of China (Grant Nos. 60838004 and 61078028), the Foundation for the Author of National Excellent Doctoral Dissertation (Grant No. 2007B34), the Program for New Century Excellent Talents in University (Grant No. NCET-07-0597), the Russian Foundation for Basic Research (projects 08-02-92226, 10-02-91173, 09-02-12373, 09-02-12359, and 09-02-92119) and the Federal Program of the Russian Ministry of Education and Science (contracts 1130 and 02.740.11.0223).

References

[1] Knight, J.C.; Birks, T.A.; Cregan, R.F.; Russell, P.S.J.; de Sandro, P.D. *Electron. Lett.* **1998,** *34,* 1347–1348.

[2] Furusawa, K.; Malinowski, A.; Price, J.; Monro, T.; Sahu, J.; Nilsson, J.; Richardson, D. *Opt. Express* **2001,** *9,* 714–720.

[3] Eidam, T.; Hanf, S.; Seise, E.; Andersen, T.V.; Gabler, T.; Wirth, C.; Schreiber, T.; Limpert, J.; Tünnermann, A. *Opt. Lett.* **2010,** *35,* 94–96.

[4] Zaouter, Y.; Boullet, J.; Mottay, E.; Cormier, E. *Opt. Lett.* **2008,** *33,* 1527–1529.

[5] Fang, X.-H.; Hu, M.-L.; Liu, B.-W.; Chai, L.; Wang, C.-Y.; Zheltikov, A.M. *Opt. Lett.* **2010,** *35,* 2326–2328.

[6] Fang, X.-H.; Hu, M.-L.; Li, Y.-F.; Chai, L.; Wang, C.-Y.; Zheltikov, A.M. *Opt. Lett.* **2010,** *35,* 493–495.

[7] Wrage, M.; Glas, P.; Fisher, D.; Leitner, M.; Vysotsky, D.V.; Napartovich, A.P. *Opt. Lett.* **2000,** *25,* 1436–1438.

[8] Wrage, M.; Glas, P.; Leitner, M. *Opt. Lett.* **2001,** *26,* 980–982.

[9] Cheo, P.K.; Liu, A.; King, G.G. *IEEE Photonics Technol. Lett.* **2001,** *13,* 439–441.

[10] Michaille, L.; Taylor, D.M.; Bennett, C.R.; Shepherd, T.J.; Ward, B.G. *Opt. Lett.* **2008,** *33,* 71–73.

[11] Li, L.; Schulzgen, A.; Li, H.; Temyanko, V.L.; Moloney, J.V.; Peyghambarian, N. *J. Opt. Soc. Am. B* **2007,** *24,* 1721–1728.

[12] Paurisse, M.; Hanna, M.; Druon, F.; Georges, P. *Opt. Lett.* **2010,** *35,* 1428–1430.

[13] Daniault, L.; Hanna, M.; Lombard, L.; Zaouter, Y.; Mottay, E.; Goular, D.; Bourdon, P.; Druon, F.; Georges, P. *Opt. Lett.* **2011,** *36,* 621–623.

[14] Fang, X.-H.; Hu, M.-L.; Liu, B.-W.; Chai, L.; Wang, C.-Y.; Wei, H.-F.; Tong, W.-J.; Luo, J.; Sun, C.-K.; Voronin, A.A.; Zheltikov, A.M. submitted for publication, 2011.

[15] Luan, F.; George, A.K.; Hedley, T.D.; Pearce, G.J.; Bird, D.M.; Knight, J.C.; Russell, P.St. *J. Opt. Lett.* **2004,** *29,* 2369–2371.

[16] Isomäki, A.; Okhotnikov, O.G. *Opt. Express* **2006,** *14,* 9238–9243.

[17] Kibler, B.; Martynkien, T.; Szpulak, M.; Finot, C.; Fatome, J.; Wojcik, J.; Urbanczyk, W.; Wabnitz, S. *Opt. Express* **2009,** *17,* 10393–10398.

[18] Bétourné, A.; Kudlinski, A.; Bouwmans, G.; Vanvincq, O.; Mussot, A.; Quiquempois, Y. *Opt. Lett.* **2009,** *34,* 3083–3085.

[19] Fedotov, I.V.; Lanin, A.A.; Voronin, A.A.; Fedotov, A.B.; Zheltikov, A.M.; Egorova, O.N.; Semjonov, S.L.; Pryamikov, A.D.; Dianov, E.M. *J. Mod. Opt.* **2010,** *57,* 1867–1870.

[20] Agrawal, G.P.*Nonlinear Fiber Optics*, 4th ed.; Academic: San Diego, 2007.

[21] Voronin, A.A.; Fedotov, I.V.; Fedotov, A.B.; Zheltikov, A.M. *Opt. Lett.* **2009,** *34,* 569–571.

[22] Zheltikov, A.M. *Phys.-Usp.* **2006,** *49,* 605–628.